Available online at www.sciencedirect.com
SCIENCE DIRECT
Biochemical and Biophysical Research Communications 346 (2006) 242–251
BBRC
www.elsevier.com/locate/ybbrc

Antitumor quinols: Role of glutathione in modulating quinol-induced apoptosis and identification of putative cellular protein targets ☆

Eng-Hui Chew [a,b], Charles S. Matthews [a], Jihong Zhang [a,1], Andrew J. McCarroll [a], Thilo Hagen [b], Malcolm F.G. Stevens [a], Andrew D. Westwell [a,2], Tracey D. Bradshaw [a,*]

[a] *Centre for Biomolecular Sciences, School of Pharmacy, University of Nottingham, Nottingham, UK*
[b] *Wolfson Digestive Diseases Centre, University of Nottingham, Nottingham, UK*

Received 16 May 2006
Available online 26 May 2006

Abstract

Novel heteroaromatic quinols 4-(benzothiazol-2-yl)-4-hydroxycyclohexa-2,5-dienone (**1**) and 4-(1-benzenesulfonyl-1*H*-indol-2-yl)-4-hydroxycyclohexa-2,5-dienone (**2**) are promising novel anticancer agents. They exhibit in vitro antiproliferative activity against colon, renal, and breast carcinoma cell lines as well as in vivo antitumor activity in colon, renal, and breast tumor xenografts. Elucidation of the mechanism of antitumor action of these compounds is of great importance. We show in this study that the compounds induced apoptosis as demonstrated by caspase 3 and PARP cleavage at doses causing G_2/M cell cycle arrest. Glutathione was found to play an important role in modulating quinol-mediated cytotoxicity. In HCT 116 cells, treatment with **1** and **2** caused a 2- to 3-fold increase in the total glutathione content, suggestive of a glutathione-mediated antioxidant response. Indeed, buthionine sulfoximine (BSO)-induced glutathione depleted cells were 6–10 times more sensitive to **1** and **2**, while glutathione monoethyl ester supplementation decreased the antitumor potencies by 2–3 times. In further studies we determined other cellular proteins which bind to an immobilized quinol analog, and identified several proteins including β-tubulin, heat shock protein 60, and peroxiredoxin 1 as potential molecular targets of quinols that may contribute to their proapoptotic and antiproliferative effects.

Keywords: Quinols; Glutathione; BSO; Apoptosis induction

A novel series of heteroaromatic-substituted hydroxycyclohexadienones (quinols) synthesized in our laboratory has been evaluated for in vitro antitumor activity. Structure-activity relationship studies have identified **1** [AW464; 4-(benzothiazol-2-yl)-4-hydroxycyclohexa-2,5-dienone] and **2** [BW114; 4-(1-benzenesulfonyl-1*H*-indol-2-yl)-4-hydroxycyclohexa-2,5-dienone] as lead compounds [1,2] (Fig. 1). In the National Cancer Institute (NCI) Development Therapeutics Program in vitro screen of 60 human-derived cancer cell lines, these molecules exhibit selective growth inhibitory activity concentrated in the colon, renal, and certain breast cell lines; **2** possesses greater growth inhibitory potency than **1** [3]. In vivo antitumor activity of **1** and **2** has also been demonstrated in renal, colon, and breast tumor xenografts [1,2]. Thioredoxin-1 (Trx-1) has recently been identified as a target for these compounds

☆ *Abbreviations:* BNIP3, BCL2 adenovirus E1B 19 kDa interacting protein 3; BSO, L-buthionine (S,R) sulfoximine; CA-IX, carbonic anhydrase-IX; CAD, C-terminal transactivation domain; EDAC, 1-ethyl-3-(3-dimethylaminopropyl)carbodiimide hydrochloride; EF-1-γ, translation elongation factor 1γ; GCL, glutamate–cysteine ligase; GSHEt, glutathione monoethyl ester; H_2DCFDA, 2′,7′-dichlorodihydrofluorescein diacetate; HIF-1α, hypoxia-inducible factor 1α; HSP60, heat shock protein 60; MALDI-TOF, matrix-assisted laser desorption/ionization time-of-flight; MTT, 3-(4,5-dimethylthiazol-2-yl)-2,5-diphenyltetrazolium bromide; NF-κB, nuclear factor κB; Prx1, peroxiredoxin 1; ROS, reactive oxygen species; Trx, thioredoxin; VEGF, vascular endothelial growth factor.

Note: This article represents part 5 in the series "Quinols as novel therapeutic agents".

* Corresponding author. Fax: +44 115 9513412.
E-mail address: tracey.bradshaw@nottingham.ac.uk (T.D. Bradshaw).
[1] J. Zhang is a visiting scholar from the Department of Pharmacy, First People's Hospital of Yunnan Province, Kunming, PR China.
[2] Present address: Welsh School of Pharmacy, Cardiff University, Cardiff, UK.

0006-291X/$ - see front matter © 2006 Elsevier Inc. All rights reserved.
doi:10.1016/j.bbrc.2006.05.106

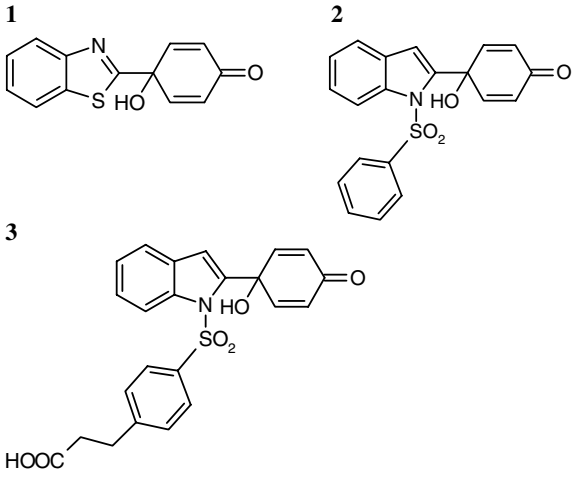

Fig. 1. Chemical structures of heteroaromatic-substituted hydroxycyclohexadienone **1** and (arylsulfonyl) indole-substituted quinols **2** and **3**.

[3], suggesting that the mechanism/s of action of these compounds is likely to involve changes in the redox state of protein thiols.

The redox state of cellular proteins is under the rigorous regulation of oxidants, reactive oxygen species (ROS), and redox buffers glutathione (GSH) and thioredoxin (Trx). GSH, the most abundant intracellular thiol molecule, serves as an antioxidant to detoxify ROS and is involved in the detoxification of endogenous and exogenous toxins through formation of GSH conjugates [4]. The dithiol-disulfide oxidoreductase property of 12 kDa Trx, mediated through its active site cysteine residues, serves to protect cellular proteins against oxidative insult, which consequentially identifies the thiol protein as having several roles critical for cellular functions. For example, in cell signaling, Trx-1 exerts redox control over several transcription factors to modulate their DNA binding activities. For instance, through reduction of a cysteine residue in the p50 subunit of nuclear factor κB (NF-κB) [5], Trx-1 activates NF-κB in the nucleus to increase DNA binding [6]. The transcription factor hypoxia-inducible factor 1α (HIF-1α) is induced in response to hypoxic conditions. In hypoxic tumors, HIF-1α expression activates the transcription of genes involved in angiogenesis, glucose metabolism, pH regulation, and others, leading to adaptive mechanisms which contribute to tumor survival and progression [7,8]. It has been reported that in cells overexpressing Trx-1, HIF-1α and vascular endothelial growth factor (VEGF) protein levels are increased under both normoxic and hypoxic conditions [9]. Trx-1 is also found to potentiate the binding of transcription coactivator complex CBP/p300 to the C-terminal transactivation domain (CAD) of HIF-1α to increase transcriptional activity; activation is achieved through redox regulation of a cysteine residue in the CAD of HIF-1α [10]. Consistent with our previous report on Trx as a mechanistic target of quinols [3], Mukherjee et al. [11] have reported a decrease in VEGF production in hypoxic tumor cells treated with **1**. In another recent study, under hypoxia, **1** and AJM290 (a structural analog of **2** possessing a fluorine substitution at the 6-position of the indole moiety) are found to increase HIF-1α protein levels, but inhibit HIF-1α transactivation, thus decreasing in a dose-dependent manner the expression levels of downstream target genes such as VEGF, carbonic anhydrase-IX (CA-IX), and BCL2 adenovirus E1B 19 kDa interacting protein 3 (BNIP-3) [12].

As promising clinical candidates, elucidation of the mechanism of antitumor action of these compounds is of importance. We have previously shown that quinols bind to cysteine residues of Trx-1 [3], suggesting that protein thiol oxidation plays a critical role in quinol-induced apoptosis. Furthermore, we have argued that the redox protein is unlikely to be the sole target and quinols are likely to also target reactive cysteines in other cellular proteins [3]. We thus studied the role of the cellular GSH system in quinol-dependent apoptosis in two tumor cell lines (HCT 116 and MCF-7) and demonstrated that it plays an important role in regulating cytotoxicity induced by **1** and **2**. By the use of a quinol analog immobilized to a solid matrix, we also identified several cellular proteins bound to the drug, including β-tubulin, heat shock protein 60 (HSP60), and peroxiredoxin 1 (Prx1), which represent potential molecular targets for this class of novel compounds.

Materials and methods

Drugs and cell culture. **1** and **2** were synthesized in our laboratory as described previously [1,2]. The carboxylic acid-linked quinol compound **3** was synthesized using a palladium-catalyzed Sonogashira coupling/intramolecular cyclization, between (methyl-3-{4-(*N*-(2-iodophenyl)sulfamoyl)phenyl)propanoate and 4-ethynyl-4-hydroxycyclohexa-2,5-dienone, as the key step followed by ester hydrolysis. Further details on the chemical synthesis of a range of (arylsulfonyl)indole-substituted quinols using this type of methodology will be reported in due course. (S)-(+)-Camptothecin was purchased from Sigma–Aldrich (St. Louis, MO). All drugs were prepared as 10 mM stock solutions in DMSO, and stored, protected from light at 4 °C. Colon carcinoma (HCT 116 and HT29) and mammary carcinoma MCF-7 cells were maintained in RPMI 1640 medium supplemented with 10% fetal bovine serum and incubated at 37 °C in an humidified atmosphere of 95% air and 5% CO_2.

Western blot analysis of apoptosis. Whole cell lysates of control or drug-treated cells were prepared by lysing cell pellets (comprised of attached and floating cells) in lysis buffer 25 mM Tris–HCl (pH 7.5), 100 mM NaCl, 2.5 mM EDTA, 2.5 mM EGTA, 20 mM NaF, 1 mM Na_3VO_4, 20 mM sodium β-glycerophosphate, 10 mM sodium pyrophosphate, and 0.5% Triton X-100 containing freshly added protease inhibitor cocktail (Roche Diagnostics, Mannheim, Germany) and 0.1% β-mercaptoethanol. Protein concentrations were determined using a modified Bradford assay (Bio-Rad Laboratories, Hercules, CA) as described in the manufacturer's manual. Equal amounts of protein (50 μg) from each sample were separated by SDS–PAGE (10%) and electroblotted to polyvinylidene difluoride membranes. The blots were probed with a primary antibody followed by a secondary antibody conjugated to horseradish peroxidase. Polyclonal anti-caspase 3, anti-cleaved caspase 3, and anti-PARP primary antibodies were purchased from Cell Signaling Technology (Beverly, MA). Monoclonal anti-β-actin antibody, used to verify equal protein transfer, was purchased from Sigma–Aldrich. Protein levels on the blots were detected using the enhanced chemiluminescence system (Amersham Pharmacia Biotech, Little Chalfont, UK) according to the

manufacturer's instructions. Three separate sets of samples for each cell line were analyzed for each drug.

GSH measurement. Cells (3×10^6) were seeded onto 100 mm-plates and incubated overnight before treatment with **1** and **2**. Treatment at each drug concentration for a specified duration was performed in duplicate. Medium containing detached cells was collected and the attached cells were trypsinized. Attached and floating cells were pooled, pelleted, and rinsed once in ice-cold PBS, and to one of the duplicate samples (per treatment), 3% 5-sulfosalicylic acid (1 ml) was added to extract cellular GSH. The mixture was centrifuged to remove precipitated proteins, and GSH was determined by the enzymatic method of Tietze [13]. Briefly, total GSH content was assayed by following the change in absorbance at 412 nm over 6 min in a cuvette containing 0.1 M sodium phosphate, 5 mM EDTA buffer (pH 7.5), 0.6 μM 5,5′-dithiobis(2-nitrobenzoic acid), 10 μg/ml yeast GSH reductase, 0.2 mM NADPH, and 20 μl of sample in a final volume of 1 ml. GSH values were calculated from a standard curve that was generated for each experiment using known amounts of GSH (0.125–1.5 μM). Total GSH levels were then normalized for total protein content that was determined from the cell lysates prepared from the remaining duplicate samples using the modified Bradford assay (Bio-Rad Laboratories).

Cell viability assay. Cells were seeded in 96-well plates at the following densities: for the BSO-induced GSH depletion assays, 1×10^3 HCT 116 and 2×10^3 MCF-7 cells were seeded into each well, and for the GSH supplementation assays, 3×10^3 HCT 116 and 4×10^3 MCF-7 cells were seeded into each well. In the BSO-induced GSH depletion assays, BSO (10 and 25 μM) was added to HCT 116 and MCF-7 cells, respectively. After 24 h, medium was removed and cells were incubated in fresh medium containing either **1** or **2** alone (BSO-pulsed exposure) or **1** or **2** plus BSO (BSO continuous exposure). Control cells in the BSO-pulsed exposure and BSO continuous exposure treatment groups were subjected to similar BSO treatment as mentioned above in the absence of **1** or **2**. Following 72 h quinol treatment, viability was determined by reduction of 3-(4,5-dimethylthiazol-2-yl)-2,5-diphenyltetrazolium bromide (MTT) as described previously [3]. In the GSH supplementation assays, 1 mM glutathione monoethyl ester (GSHEt) was added to cells 2 h prior to **1** or **2** addition. After drug exposure for 72 h, MTT viability assays were performed.

ROS measurement. Intracellular ROS generation was assessed using the cell permeant dye 2′,7′-dichlorodihydrofluorescein diacetate (H_2DCFDA) [14]. Intracellular, membrane-bound esterases and ROS, respectively, cleave and oxidize non-fluorescent H_2DCFDA to the fluorescent 2′,7′-dichlorofluorescein (DCF). Cells were seeded (1×10^5 cells/well) in 24-well plates and allowed to adhere overnight. For the next 24 h, cells to be GSH depleted were incubated with BSO (10 and 25 μM was added to HCT 116 and MCF-7 cells, respectively), while non-GSH-depleted cells were maintained in medium only. The cells were then treated with concentrations of **1** and **2** (**1**: 0.5–5 μM, **2**: 0.2 – 3 μM) for 3–24 h at 37 °C. H_2DCFDA (final concentration 5 μM) was added for the final 30 min at 37 °C of the incubation period. Medium containing detached cells was collected and the attached cells were trypsinized. Attached and floating cells were pooled, pelleted, rinsed once in ice-cold PBS, and resuspended in 0.3 ml propidium iodide (PI: 1 μg/ml PBS) solution. Cells were kept on ice in the dark and analyzed immediately on a Beckman Coulter EPICS-XL flow cytometer (488 nm laser). DCF fluorescence was recorded in the FL1 channel (525 nm) and PI fluorescence in FL3 (620 nm). Data analysis was carried out using EXPO32 (Applied Cytometry Systems, UK). PI positive cells were considered non-viable and excluded from ROS analysis.

Plasmid constructs and transfection of HCT 116 cells. The full-length coding sequences of HSP60 and Prx1, including a C-terminal V5 and 2× Flag tag, respectively, were PCR-amplified from human cDNA (derived from HEK293 cells), and cloned into the *Kpn*I and *Xba*I sites of pcDNA3 expression vector (Invitrogen, Paisley, UK). Sub-confluent HCT 116 cells grown in 100 mm-plates were transfected with pcDNA3HSP60-V5 or pcDNA3Prx1-Flag (5 μg) using GeneJuice (Novagen, Nottingham, UK) as the transfection reagent.

Drug immobilization, in vitro binding, and protein spot analysis. For drug immobilization, 10 mg 1-ethyl-3-(3-dimethylaminopropyl) carbodiimide hydrochloride (EDAC) and compound **2** or **3** (final concentration 2 mM; Fig. 1), or DMSO vehicle alone were added to 150 μl Affi-Gel 102 (amino-terminal crosslinked agarose beads, Bio-Rad Laboratories) diluted with 50 μl DMSO. After incubation at room temperature for 4 h, the beads were washed four times in cold PBS. HCT 116 cells grown in six 100 mm-plates were lysed in lysis buffer with a composition as described above, but β-mercaptoethanol was omitted. The lysates were clarified by centrifugation, and the pooled supernatants were divided and incubated with the beads at 4 °C for 16 h. The beads were washed six times with a buffer solution containing 1 M NaCl, 20 mM Tris–HCl (pH 7.5), and 1 mM EGTA. Bound proteins were recovered by boiling in SDS–PAGE sample buffer containing 100 mM DTT for 30 min. The proteins were separated by SDS–PAGE on a 12% polyacrylamide gel (120 × 120 mm), fixed, and Coomassie stained (40% methanol, 10% acetic acid, and 1% Coomassie blue) for 15 min. The experiment was repeated twice and gel bands commonly identified in repeated gels were excised and placed in a 96-well plate. The plate was loaded onto the automated MassPrep robotic liquid handling system (Waters Corp/Bio-Rad ProteomeWorks). Briefly, gel pieces were destained in 50% acetonitrile in 50 mM ammonium bicarbonate (NH_4HCO_3). The cysteine residues were reduced in 10 mM DTT in 100 mM NH_4HCO_3, followed by alkylation in 55 mM iodoacetamide in 100 mM NH_4HCO_3. The gel pieces were dehydrated by acetonitrile, and subjected to in-gel tryptic digestion (6 ng/μl trypsin in 50 mM NH_4HCO_3, pH 8.0) for 3 h at 37 °C. Peptides were extracted in 1% formic acid in 2% acetonitrile. C18 loaded zip-tips (Millipore Corp, Bedford, MA) were used to load 2 μl of the peptide extracts with 1 μl of matrix solution (α-cyano-4-hydroxycinnaminic acid) onto the wells of a stainless steel MALDI target plate. MALDI-TOF analyses of peptide fragments were carried out using a Waters MALDI-TOF mass spectrometer (Waters Corp, Milford, MA) operating in reflectron mode. Proteins were identified by analyzing peptide mass fingerprints using the MASCOT PMF database search engine (www.matrixscience.com). Search parameters included a peptide mass accuracy tolerance of 0.2 Da and possible modifications such as alkylation of cysteine residues during tryptic digestion and oxidation of methionine residues were allowed. To verify the in vitro binding of two of the identified proteins, pooled lysates from four 100 mm-plates of HCT 116 cells transfected (48 h) with pcDNA3HSP60-V5 or pcDNA3Prx1-Flag were divided and incubated with beads coupled with or without compound **3**. Bound proteins eluted (by boiling) into sample buffer were separated by SDS–PAGE and electroblotted to polyvinylidene difluoride membranes. Protein levels of HSP60-V5 and Prx1-Flag were analyzed by Western blotting. Monoclonal anti-V5 (Serotec, Oxford, UK) and anti-Flag (Sigma–Aldrich) antibodies were used.

Statistical analyses. For assays measuring ROS production and total GSH levels, unpaired Student's *t* tests were used to assess differences between quinol-treated and control groups. For viability assays determining the sensitivity of cells to quinols, paired Student's *t* tests were used to assess differences between BSO-/GSHEt-treated and untreated groups. A p value of <0.05 was considered statistically significant.

Results

Quinols induce caspase-dependent apoptosis

The caspase-dependent mode of cell death for quinols was first reported in HL60 leukemia cells where pan-caspase inhibitor z-VAD-FMK inhibited apoptosis induced by **1** [15]. In the epithelial HCT 116 colon cancer cell line, as measured by annexin V/PI staining, a similar inhibitory effect of z-VAD-FMK (50 μM) on apoptosis induced by **1** and **2** was observed (results not shown). Induction of caspase-dependent apoptosis in quinol-sensitive cell lines (HCT 116, HT29, and MCF-7) was confirmed by positive immunodetection of cleaved caspase 3 (17 and 19 kDa) and PARP (89 kDa). As illustrated in Fig. 2A–C, **1** and **2**

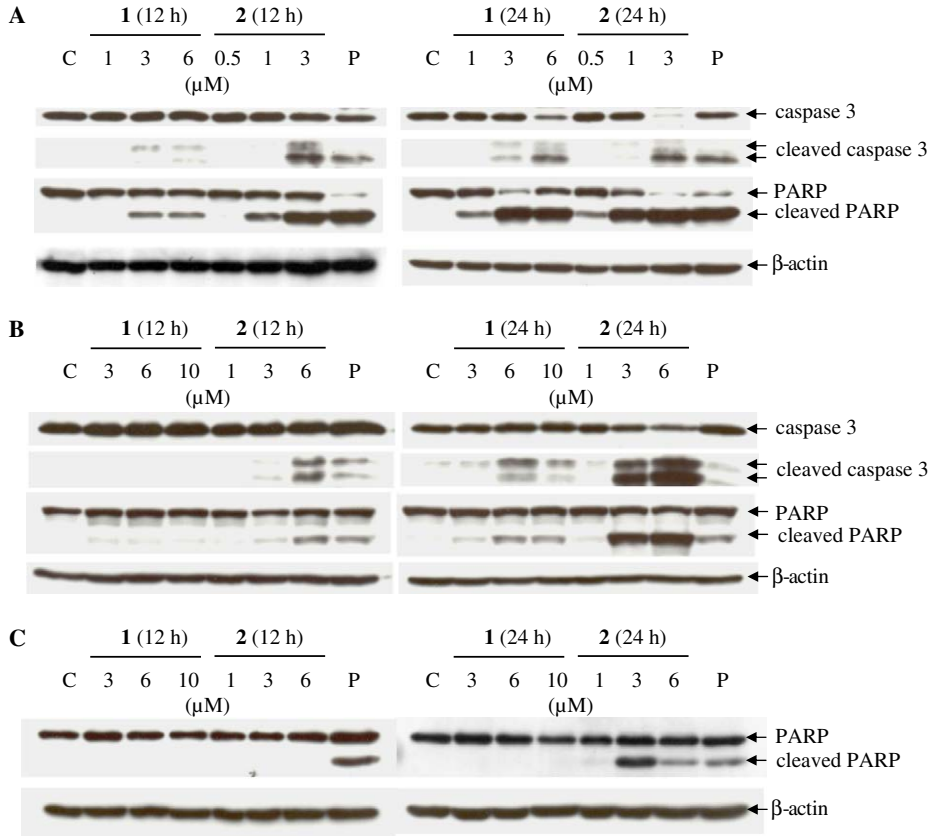

Fig. 2. Western blot analysis of caspase 3 and PARP cleavage induced by **1** and **2**. HCT 116 (A), HT29 (B), and MCF-7 (C) cells were treated with the indicated concentrations of **1** and **2** for 12 or 24 h. Whole cell lysates were subjected to Western blotting with the indicated antibodies, showing that **1** and **2** caused a dose- and time-dependent increase in caspase 3 and/or PARP cleavage. C, control cells; P, positive control: cells were treated with camptothecin (1 μM) for 24 h.

caused a dose- and time-dependent increase in caspase 3 and PARP cleavage, with **2** being presented as the more potent analog. The topoisomerase I inhibitor (S)-(+)-Camptothecin (1 μM) was used as a positive control. The Western blot results correlated with the previously reported irreversible G_2/M cell cycle arrest induced by **1** and **2** and their antiproliferative potencies [3], where G_2/M block and cytotoxicity were most pronounced in the most sensitive HCT 116 cells. In contrast, in caspase 3-deficient MCF-7 cells (Fig. 2C), **1** failed to induce PARP cleavage within 24 h at all tested concentrations (3–10 μM), while **2** induced PARP cleavage at higher doses ($\geqslant 3$ μM) at a delayed time of 24 h.

Cytoprotective role of GSH in quinol-induced cytotoxicity

To assess effects of quinol treatment on the GSH system, total intracellular GSH levels were quantified following 7 and 24 h exposure to **1** and **2**. As shown in Fig. 3, treatment of HCT 116 and MCF-7 cells with **1** and **2** resulted in a time-dependent increase in GSH content. At an early time point of 7 h, the rise was marginal, particularly in MCF-7 cells (Fig. 3B), where either an insignificant ($p < 0.05$) increase or a transient decline caused by treatment with a high dose of **1** (6 μM) was observed. By 24 h, 2- to 3-fold enhanced GSH levels were detected (Fig. 3A and B). Elevation in total GSH content indicated a cellular antioxidant response evoked by drug entry. To further discern the cytoprotective role of GSH, MTT viability assays were carried out to determine whether modulation of GSH levels would affect cell sensitivity to **1** and **2**. As cell lines exhibit differential degrees of GSH depletion, a nontoxic BSO dose to bring about sufficient GSH depletion was predetermined. Fig. 4A and B show the dose-response graph (representative of four separate MTT assays) for HCT 116 and MCF-7 cells (respectively) subjected to 96 h treatment with BSO (0.5–500 μM). A respective BSO dose of 10 and 25 μM was identified to achieve effective GSH depletion (HCT 116 cells: 86%, MCF-7 cells: 80%) after 24 h treatment. As shown in Table 1A, cells depleted of GSH by continuous exposure to BSO were 6- to 10-fold more sensitive to **1** and **2**. For cells receiving BSO pulsed treatment, there was no significant enhancement ($p > 0.05$) in quinol potency, with the exception seen with HCT 116 cells treated with **2** where a twofold increase in cell sensitivity was evident ($p < 0.05$, Table 1A). Conversely, cellular GSH supplementation cells caused a 2- to 3-fold decline in quinol antitumor potency (Table 1B). Taken together, these results suggest that GSH plays an important role in cell survival against the cytotoxic effects of **1** and **2**.

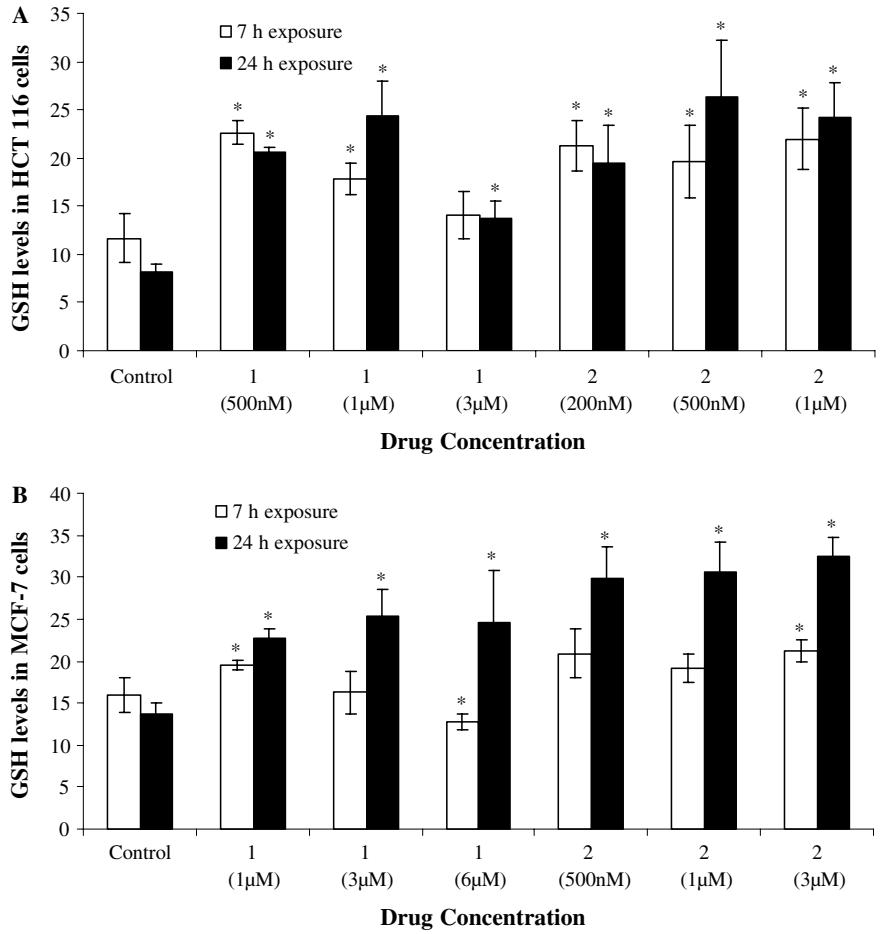

Fig. 3. Total GSH levels in HCT 116 (A) and MCF-7 (B) cells exposed to **1** and **2**. Cells were treated with **1** and **2** for 7 and 24 h and the cellular GSH content (nmol/mg protein) was determined. Each data point was obtained from the average of three independent experiments. A time-dependent increase was observed in both cell lines: at 7 h, the levels either rose marginally or decreased transiently, and by 24 h, the levels at all tested concentrations were significantly increased ($p < 0.05$, denoted as an asterisk *) by 2- to 3-fold.

Quinols induce transient ROS production that is not enhanced by GSH depletion

To determine whether quinols induce ROS production, we examined the effect of **1** and **2** on the cellular levels of H_2O_2 using H_2DCFDA as a fluorescent probe. In the assay, as necrotic and late apoptotic cells were PI counterstained and excluded from fluorescence analysis, the measured fluorescence intensity was contributed by H_2O_2 accumulation in live and early apoptotic cells. Fig. 5 shows the percentage of DCF fluorescence in drug-treated cells over that in DMSO control cells. Of the two cell lines tested, MCF-7 cells failed to evoke a statistically significant increase in ROS production in response to all tested concentrations of **1** and **2** at the specified time points. In HCT 116 cells, significantly higher ($p < 0.05$) ROS levels were brought about by **1** (3 and 5 μM at 3 h, 5 μM at 7 h) and **2** (0.5, 1, and 3 μM at 3 h), although it may be appreciated from the data that increased ROS generation occurred transiently: levels peaked within 3–7 h quinol exposure and were normalized by 24 h. A similar trend was evident in MCF-7 cells, where ROS levels were lower (in response to **1**, Fig. 5A) or comparable (in response to **2**, Fig. 5B) to levels detected in control cells at the 24 h time point. We further measured ROS levels induced by **1** and **2** in GSH-depleted cells. Treatment of HCT 116 cells with BSO (10 μM) for 24 h caused twofold increase in DCF fluorescence ($p < 0.05$) (Fig. 5C). However, there was no significant net gain ($p > 0.05$) in DCF fluorescence measured in these GSH-depleted cells treated with **1** (0.5, 1, 3, and 5 μM) and **2** (0.2, 0.5, 1, and 3 μM) at all time points examined. For illustration, data obtained for cells incubated with a high dose of **1** and **2** (3 μM) are presented in Fig. 5C. Similar results were observed with MCF-7 cells (results not shown). The data suggest that quinol-induced ROS formation is not enhanced by GSH depletion.

Other cellular proteins as potential molecular targets of quinols

To explore potential protein targets of quinols, compound **3** (Fig. 1), a carboxylic acid derivative of **2**, was synthesized. By means of the use of the coupling agent EDAC, **3** was immobilized onto the aminoalkyl agarose beads via

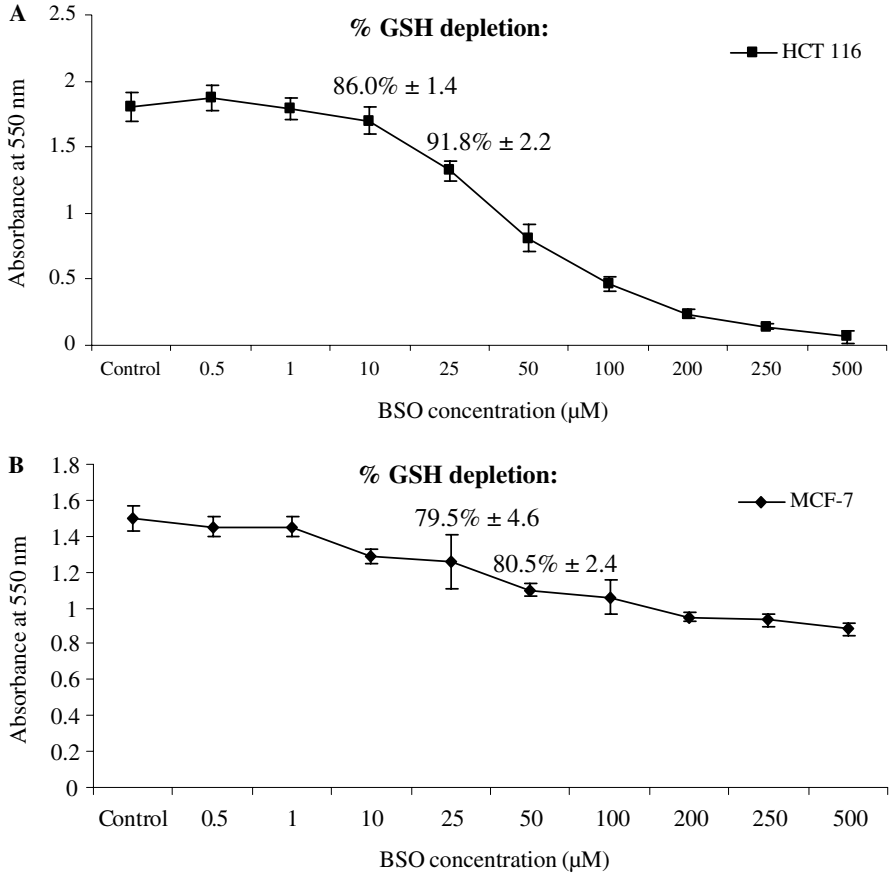

Fig. 4. In vitro toxicity profile of BSO. HCT 116 (A) and MCF-7 (B) cells were exposed to BSO at various concentrations for 96 h prior to viability determination by MTT assay. Points are means of 4-well readings on a single experiment. Experiments were done on four separate occasions. Extent of GSH depletion was quantified following 24 h of treatment with two selected BSO concentrations. BSO doses of 10 and 25 μM that produced minimum toxicity and effective GSH depletion on HCT 116 and MCF-7 cells, respectively, were chosen for subsequent assays.

Table 1
Growth inhibitory activity of **1** and **2** against HCT 116 and MCF-7 cells treated or untreated with (A) BSO or (B) GSHEt

A	GI_{50} values (nM) of **1** and **2** evaluated on					
	HCT 116 cells			MCF-7 cells		
	No BSO	Pulsed BSO	Continuous BSO	No BSO	Pulsed BSO	Continuous BSO
1	440 ± 56	366 ± 49 ($p > 0.05$)	46 ± 13 ($p < 0.05$)	544 ± 12	427 ± 88 ($p < 0.05$)	52 ± 19 ($p < 0.05$)
2	239 ± 82	112 ± 63 ($p > 0.05$)	22 ± 11 ($p < 0.05$)	345 ± 128	301 ± 164 ($p > 0.05$)	57 ± 16 ($p < 0.05$)

B	GI_{50} values (nM) of **1** and **2** evaluated on			
	HCT 116 cells		MCF-7 cells	
	No GSHEt	GSHEt	No GSHEt	GSHEt
1	194 ± 101	578 ± 164 ($p < 0.05$)	275 ± 95	885 ± 352 ($p < 0.05$)
2	104 ± 21	205 ± 33 ($p < 0.05$)	165 ± 75	265 ± 96 ($p < 0.05$)

(A) Cells pretreated with BSO (24 h) were exposed to **1** and **2** for 72 h either without (pulsed treatment) or in the continuous presence (continuous treatment) of BSO. (B) GSHEt (1 mM) was added to cells 2 h prior to treatment (72 h) with **1** and **2**. GI_{50} values are presented as means ± SD from 4 independent experiments. A paired Student's *t* test was performed to determine the *p* value (given in parentheses) in each treatment (BSO/GSHEt treated) group.

an amide linkage formed between the carboxyl group on **3** and the free amino group at the terminal of the hydrophilic arm of the beads. Protein bands reproducible on three repeated Coomassie-stained gels were excised, in-gel digested with trypsin, and identified by MALDI-TOF as HSP60, β-tubulin, translation elongation factor 1γ (EF-1-γ), β-actin, 40 S ribosomal protein, and Prx1 (Fig. 6A, lane 3). Two negative controls were used: one with lysate incubated with beads uncoupled to any drug and another with lysates incubated with beads pretreated with **2** and EDAC

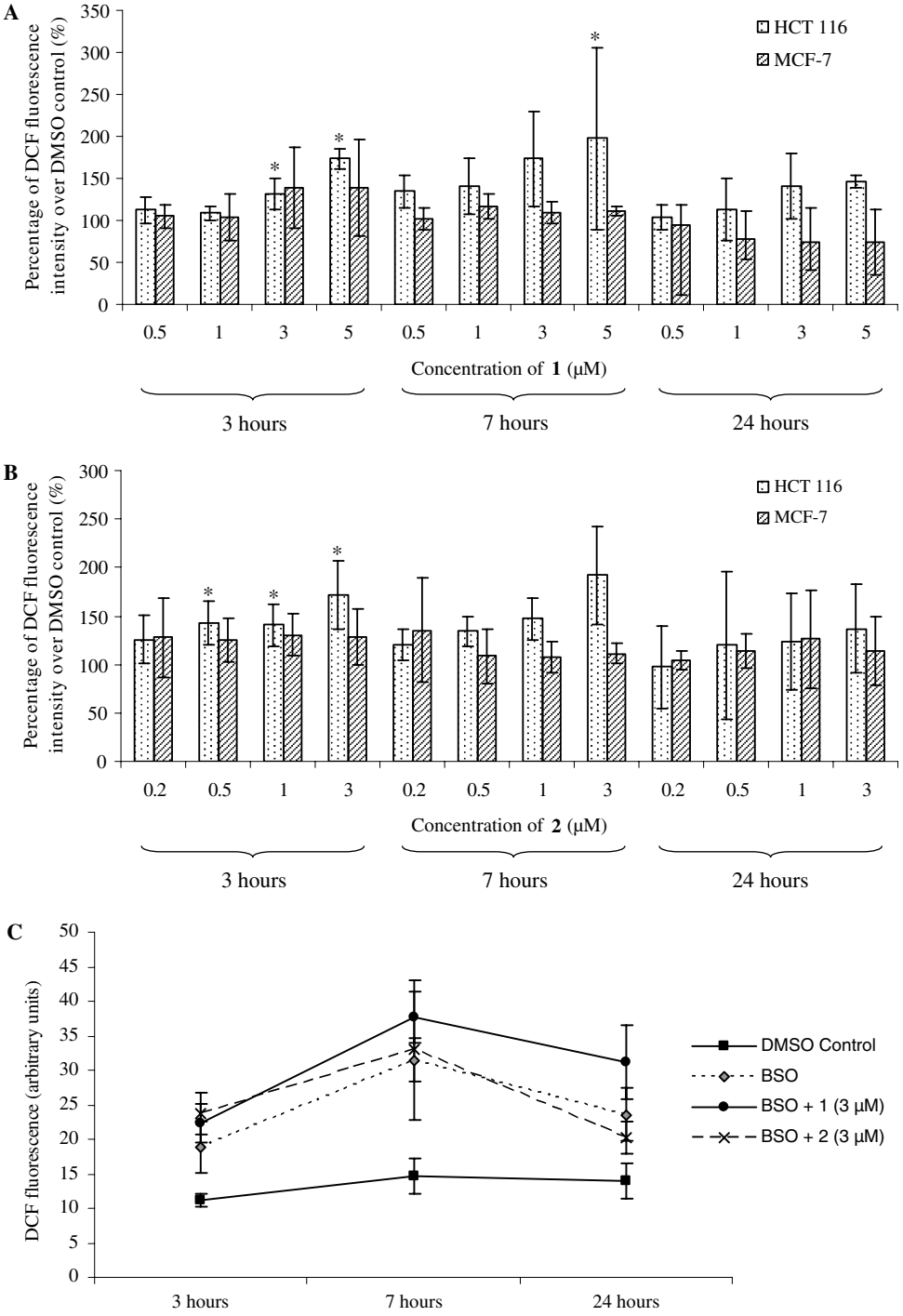

Fig. 5. ROS levels produced in HCT 116 and MCF-7 cells following exposure to **1** and **2**. (A) Levels of ROS detected in cells treated with **1** were expressed as percentage of DCF fluorescence in each drug-treated sample over that in the corresponding DMSO control sample. Differences in ROS levels (from three independent experiments) between the two sample groups were analyzed by Student's t test. Significant ROS formation ($p < 0.05$), denoted as an asterisk (∗), was seen in HCT 116 cells treated with high doses of **1** (3 and 5 μM at 3 h, 5 μM at 7 h). (B) Similar experiment with **2**, with significant ROS formation ($p < 0.05$) observed in HCT 116 cells exposed to **2** (0.5, 1, and 3 μM) for 3 h. (C) HCT 116 cells depleted of GSH by preincubation (24 h) with BSO (10 μM) were treated or untreated with **1** and **2** (3 μM) for 3, 7 or 24 h in the continuous presence of BSO. In comparison with DMSO control, treatment with BSO alone caused an increase in DCF fluorescence by around twofold ($p < 0.05$) ($n = 3$). No significant net gain ($p > 0.05$) ($n = 3$) in DCF fluorescence was observed between cells treated with BSO alone and cells treated with BSO + **1** or **2**. Similar results were observed with the MCF-7 cells (results not shown).

(Fig. 6A, lanes 2 and 1, respectively). As neither involved drug immobilization, we observed no or faint protein bands (as a result of nonspecific binding of proteins directly to the beads). In order to verify the in vitro binding of two of the proteins identified from the gel, lysates of HCT 116 cells expressing HSP60-V5 or Prx1-Flag protein were

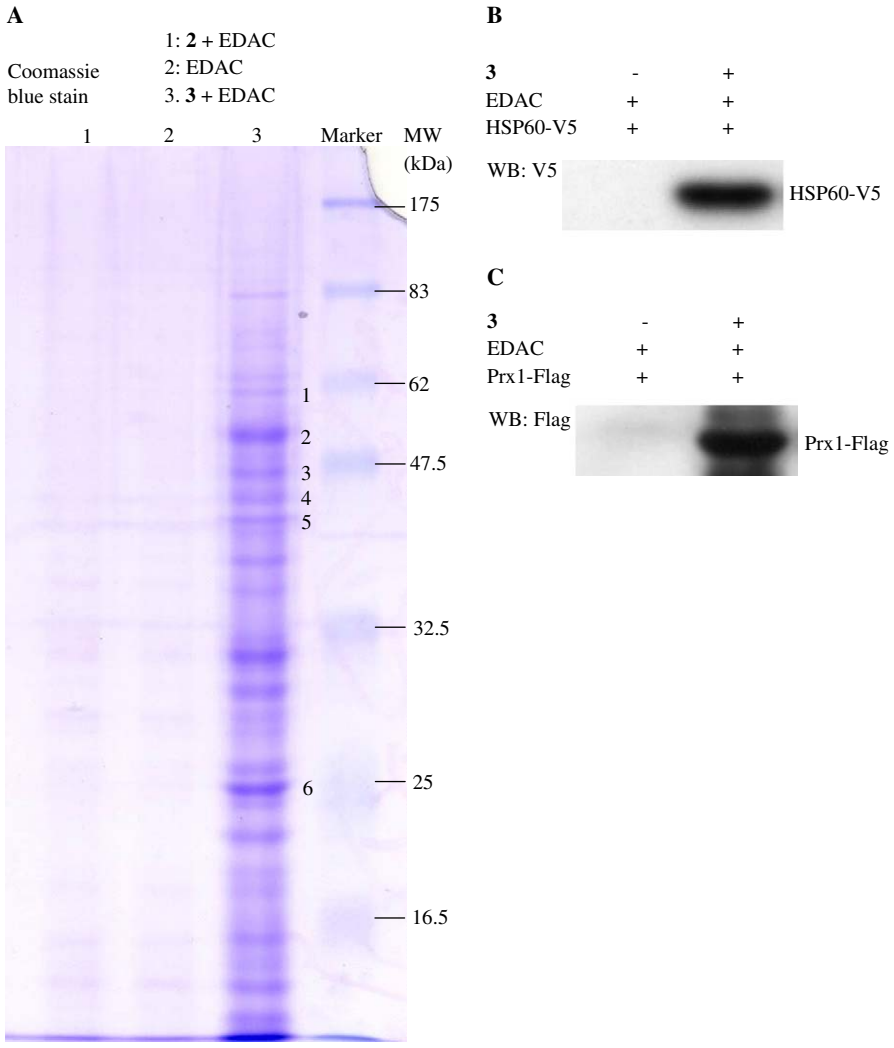

Fig. 6. Identification of cellular proteins as molecular targets of quinols. (A) Compound **3** was immobilized onto aminoalkyl agarose beads and the beads were incubated with whole cell lysates of HCT 116 cells. Bound proteins were separated by SDS–PAGE and the gel was Coomassie stained. Gel bands commonly identified in repeated gels were excised, in-gel digested, and subjected to MALDI-TOF analysis. Proteins identified in lane 3 of the gel shown were 1, HSP60; 2, β-tubulin; 3, EF-1-γ; 4, β-actin; 5, 40S ribosomal protein; 6, Prx1. Lane 1: negative control, where agarose beads were pretreated with compound **2** and EDAC. Lane 2: negative control, where agarose beads were drug-uncoupled. The gel presented is representative of three separate analyses. (B) Whole cell lysates of HCT 116 cells expressing HSP60-V5 were incubated with beads coupled or uncoupled to **3**. Western blot analysis using anti-V5 antibody only detected presence of HSP60-V5 bound to quinol-coupled beads. (C) Whole cell lysates of HCT 116 cells expressing Prx1-Flag were incubated with beads coupled or uncoupled to **3**. Western blot analysis using anti-Flag antibody only detected presence of Prx1-Flag bound to quinol-coupled beads.

incubated with beads either coupled or uncoupled to **3**, and bound proteins were examined by immunoblotting using anti-V5 or anti-Flag antibodies that specifically recognized the proteins of interest. Western blots showed that HSP60-V5 (Fig. 6B) and Prx1-Flag (Fig. 6C) bound to the quinol-coupled but not to control beads.

Discussion

In vitro screening of a series of heteroaromatic-substituted quinol analogs (bearing a common hydroxycyclohexadienone pharmacophore) against the NCI 60 human cancer cell line panel demonstrated cytotoxicity in colon, renal, and certain breast carcinoma cell lines [1–3]. Previous work focusing on lead quinols **1** and **2** has reported their ability to induce G_2/M cell cycle arrest at growth inhibitory concentrations [3]. Here, we report the apoptosis inducing potential of **1** and **2**, as evident from the detection of caspase 3 and PARP cleavage, at concentrations which evoke irreversible G_2/M cell cycle arrest. With respect to the susceptibility of the investigated cell lines to quinols, our studies showed consistency in the degree of G_2/M block and apoptosis induction, which was most profound in the most sensitive HCT 116 cells.

To achieve a deeper understanding of the biological effects exerted by quinols, we carried out experiments on HCT 116 and MCF-7 cells, which comprised a model of quinol-sensitive and -less sensitive tumor cells. In view of the chemically reactive nature of quinols as Michael acceptors and the identification of the redox protein Trx as a

putative target [3], we assessed the role of GSH in quinol-induced cytotoxicity. The observed time-dependent increase in intracellular GSH levels in cells treated with **1** and **2** is indicative of a GSH-mediated response. To clarify the possible cytoprotective role of GSH, GSH depleted (using BSO) or supplemented cells were treated with **1** and **2**, and viability assays were performed. Continuous BSO treatment increased the potency of **1** and **2** 6- to 10-fold. In contrast, pulsed BSO treatment was without effect, with the exception of HCT 116 cells treated with **2** where a twofold increase in cell sensitivity was evident. The lack of an effect with pulsed BSO addition is likely to be due to BSO not being an irreversible inhibitor of glutamate–cysteine ligase (GCL) and after BSO washout, GSH synthesis could recover sufficiently. Therefore, it is proposed that in BSO-pulsed HCT 116 cells (displaying greater sensitivity to quinols) challenged with the more potent quinol compound **2**, the transiently impaired GSH system failed to recover in time, leading to the enhanced potency observed. GSH supplementation resulted in a 2- to 3-fold decrease in the potencies of **1** and **2**. Taken together, our results indicate that the GSH system plays an important role in quinol-induced apoptosis, which is consistent with the hypothesis that oxidation of protein thiols is a critical event in the mechanism/s of action of these antitumor quinol compounds.

Whereas **1** and **2** failed to evoke oxidative stress in the less quinol-sensitive MCF-7 cell line, increased ROS generation occurring at an early onset of 3 h drug treatment was observed in HCT 116 cells. Consistent with the findings of studies conducted on other human cell types [16,17], BSO-induced GSH depletion resulted in a significant increase in ROS production. However, quinol treatment of these GSH-depleted cells failed to enhance further levels of ROS. The data thus suggest that, although ROS production may account for the greater sensitivity of HCT 116 cells, antitumor quinols do not appear to depend exclusively on ROS generation to execute cytotoxicity but may directly induce protein thiol oxidation that is counteracted by GSH.

As the results suggest that other protein targets may account for the proapoptotic and antiproliferative effects of quinols, we employed mass spectrometry to identify cellular proteins bound to a quinol agent that had been immobilized onto aminoalkyl agarose beads. For these studies, we used compound **3**, which is identical to **2** except for a carboxyethyl group that is not expected to affect the interaction of the hydroxycyclohexadienone pharmacophore with potential target proteins. Interestingly, we observed an overlap of drug bound proteins identified in our study, and proteins detected to undergo intra- or intermolecular disulfide bond formation under prooxidant conditions caused by diamide treatment [18]. These proteins include β-tubulin, EF-1-γ, and Prx1. In the same work of Cumming et al. [18], a number of heat shock proteins such as HSP90 and HSP70 were also identified as disulfide-bonded proteins during oxidative stress, which is consistent with the detection of HSP60 in our study. The significant overlap suggests that the mode of quinol binding to these identified proteins is likely to be via a cross-linkage between the electrophilic positions on the quinol hydroxycyclohexadienone pharmacophore and the thiol group/s on the proteins. The precedence of demonstrated quinol binding to cysteine residues in Trx further lent support to the postulation that quinols bind to these other proteins at cysteine residues. Therefore, utilization of a quinol analog immobilized on a solid platform to investigate in vitro binding of cellular proteins led to identification of proteins as potential molecular targets of quinols. To validate the functional significance of drug binding to these proteins, experiments will be conducted to determine whether quinol binding results in inhibitory protein function and accounts for quinol-mediated cytotoxicity. In the context of cancer drug development, targeting against tubulin, HSP60, and Prx is of relevance. Like the anticancer agents paclitaxel and vincristine (known to perturb microtubule assembly and disassembly), quinols induce a G_2/M cell cycle block. Heat shock proteins participate in the correct folding and refolding of proteins [19]. The role of HSP60 in cell death has yet to be widely explored. To date, studies conducted on cardiac myocytes have reported that HSP60 and its co-chaperone HSP10 possess an antiapoptotic role [20–22]. On the contrary, it has been observed in Jurkat cells that HSP60 accelerates the activation of caspase 3 during apoptosis [23,24]. Further work to elucidate the complex role of HSP60 in apoptosis will clarify whether inhibition of HSP60 is a valid drug-targeted apoptosis pathway for cancer treatment. Prxs are a group of antioxidant enzymes that scavenge peroxides through active site cysteine residues [25]; quinols may possess Prx inhibitory activity by binding to these catalytic cysteine residues. The identified proteins thus warrant further investigation to explore the biological significance of their inhibition and their validity as targets for therapeutic intervention. Not least, these proteins may provide further clarification to the still not fully defined mode/s of action of antitumor quinols.

Acknowledgments

Grant support: Cancer Research UK (C.S.M., A.J.M., T.D.B., A.D.W., and M.F.G.S.), University of Nottingham (E.-H.C. and T.H.). This work was supported by Cancer Research UK grant to M.F.G.S. We thank Kevin Bailey and Matthew Carlile, Biopolymer synthesis and analysis unit, School of Biomedical Sciences, University of Nottingham, for the MALDI-TOF analysis.

References

[1] G. Wells, J.M. Berry, T.D. Bradshaw, A.M. Burger, A. Seaton, B. Wang, A.D. Westwell, M.F.G. Stevens, 4-Substituted 4-hydroxycyclohexa-2,5-dien-1-ones with selective activities against colon and renal cancer cell lines, J. Med. Chem. 46 (2003) 532–541.

[2] J.M. Berry, T.D. Bradshaw, I. Fichtner, R. Ren, C.H. Schwalbe, G. Wells, E.-H. Chew, M.F.G. Stevens, A.D. Westwell, Quinols as novel therapeutic agents. 2.(1) 4-(1-Arylsulfonylindol-2-yl)-4-hydroxycyclohexa-2,5-dien-1-ones and related agents as potent and selective antitumor agents, J. Med. Chem. 48 (2005) 639–644.
[3] T.D. Bradshaw, C.S. Matthews, J. Cookson, E.-H. Chew, M. Shah, K. Bailey, A. Monks, E. Harris, A.D. Westwell, G. Wells, C.A. Laughton, M.F.G. Stevens, Elucidation of thioredoxin as a molecular target for antitumor quinols, Cancer Res. 65 (2005) 3911–3919.
[4] D.A. Dickinson, H.J. Forman, Cellular glutathione and thiols metabolism, Biochem. Pharmacol. 64 (2002) 1019–1026.
[5] J.R. Matthews, N. Wakasugi, J.L. Virelizier, J. Yodoi, R.T. Hay, Thioredoxin regulates the DNA binding activity of NF-κB by reduction of a disulphide bond involving cysteine 62, Nucleic Acids Res. 20 (1992) 3821–3830.
[6] K. Hirota, M. Murata, Y. Sachi, H. Nakamura, J. Takeuchi, K. Mori, J. Yodoi, Distinct roles of thioredoxin in the cytoplasm and in the nucleus. A two-step mechanism of redox regulation of transcription factor NF-κB, J. Biol. Chem. 274 (1999) 27891–27897.
[7] A.L. Harris, Hypoxia-a key regulatory factor in tumour growth, Nat. Rev. Cancer. 2 (2002) 38–47.
[8] G.L. Semenza, HIF-1 and tumor progression: pathophysiology and therapeutics, Trends Mol. Med. 8 (2002) S62–S67.
[9] S.J. Welsh, W.T. Bellamy, M.M. Briehl, G. Powis, The redox protein thioredoxin-1 (Trx-1) increases hypoxia-inducible factor 1alpha protein expression: Trx-1 overexpression results in increased vascular endothelial growth factor production and enhanced tumor angiogenesis, Cancer Res. 62 (2002) 5089–5095.
[10] M. Ema, K. Hirota, J. Mimura, H. Abe, J. Yodoi, K. Sogawa, L. Poellinger, Y. Fujii-Kuriyama, Molecular mechanisms of transcription activation by HLF and HIF1alpha in response to hypoxia: their stabilization and redox signal-induced interaction with CBP/p300, EMBO J. 18 (1999) 1905–1914.
[11] A. Mukherjee, A.D. Westwell, T.D. Bradshaw, M.F.G. Stevens, J. Carmichael, S.G. Martin, Cytotoxic and antiangiogenic activity of AW464 (NSC 706704), a novel thioredoxin inhibitor: an in vitro study, Br. J. Cancer 92 (2005) 350–358.
[12] D.T. Jones, C.W. Pugh, M.F.G. Stevens, A.L. Harris, Novel thioredoxin inhibitors paradoxically increase HIF-1α expression but decrease functional transcriptional activity, DNA binding and degradation, Clin. Cancer Res. in press.
[13] F. Tietze, Enzymic method for quantitative determination of nanogram amounts of total and oxidized glutathione: applications to mammalian blood and other tissues, Anal. Biochem. 27 (1969) 502–522.
[14] D.A. Bass, J.W. Parce, L.R. Dechatelet, P. Szejda, M.C. Seeds, M. Thomas, Flow cytometric studies of oxidative product formation by neutrophils: a graded response to membrane stimulation, J. Immunol. 130 (1983) 1910–1917.
[15] M. Pallis, T.D. Bradshaw, A.D. Westwell, M. Grundy, M.F.G. Stevens, N. Russell, Induction of apoptosis without redox catastrophe by thioredoxin-inhibitory compounds, Biochem. Pharmacol. 66 (2003) 1695–1705.
[16] D. Wu, A. Cederbaum, Glutathione depletion in CYP2E1-expressing liver cells induces toxicity due to the activation of p38 mitogen-activated protein kinase and reduction of nuclear factor-kappaB DNA binding activity, Mol. Pharmacol. 66 (2004) 749–760.
[17] G. Filomeni, K. Aquilano, G. Rotilio, M.R. Ciriolo, Antiapoptotic response to induced GSH depletion: involvement of heat shock proteins and NF-kappaB activation, Antioxid. Redox Signal. 7 (2005) 446–455.
[18] R.C. Cumming, N.L. Andon, P.A. Haynes, M. Park, W.H. Fischer, D. Schubert, Protein disulfide bond formation in the cytoplasm during oxidative stress, J. Biol. Chem. 279 (2004) 21749–21758.
[19] F.U. Hartl, M. Hayer-Hartl, Molecular chaperones in the cytosol: from nascent chain to folded protein, Science 295 (2002) 1852–1858.
[20] K.M. Lin, B. Lin, I.Y. Lian, R. Mestril, I.E. Scheffler, W.H. Dillmann, Combined and individual mitochondrial HSP60 and HSP10 expression in cardiac myocytes protects mitochondrial function and prevents apoptotic cell deaths induced by simulated ischemia-reoxygenation, Circulation 103 (2001) 1787–1792.
[21] S.R. Kirchhoff, S. Gupta, A.A. Knowlton, Cytosolic heat shock protein 60, apoptosis, and myocardial injury, Circulation 105 (2002) 2899–2904.
[22] Y.X. Shan, T.J. Liu, H.F. Su, A. Samsamshariat, R. Mestril, P.H. Wang, Hsp10 and Hsp60 modulate Bcl-2 family and mitochondria apoptosis signaling induced by doxorubicin in cardiac muscle cells, J. Mol. Cell. Cardiol. 35 (2003) 1135–1143.
[23] A. Samali, J. Cai, B. Zhivotovsky, D.P. Jones, S. Orrenius, Presence of a pre-apoptotic complex of pro-caspase-3, Hsp60 and Hsp10 in the mitochondrial fraction of jurkat cells, EMBO J. 18 (1999) 2040–2048.
[24] S. Xanthoudakis, S. Roy, D. Rasper, T. Hennessey, Y. Aubin, R. Cassady, P. Tawa, R. Ruel, A. Rosen, D.W. Nicholson, Hsp60 accelerates the maturation of pro-caspase-3 by upstream activator proteases during apoptosis, EMBO J. 18 (1999) 2049–2056.
[25] Z.A. Wood, E. Schroder, J. Robin Harris, L.B. Poole, Structure, mechanism and regulation of peroxiredoxins, Trends Biochem. Sci. 28 (2003) 32–40.